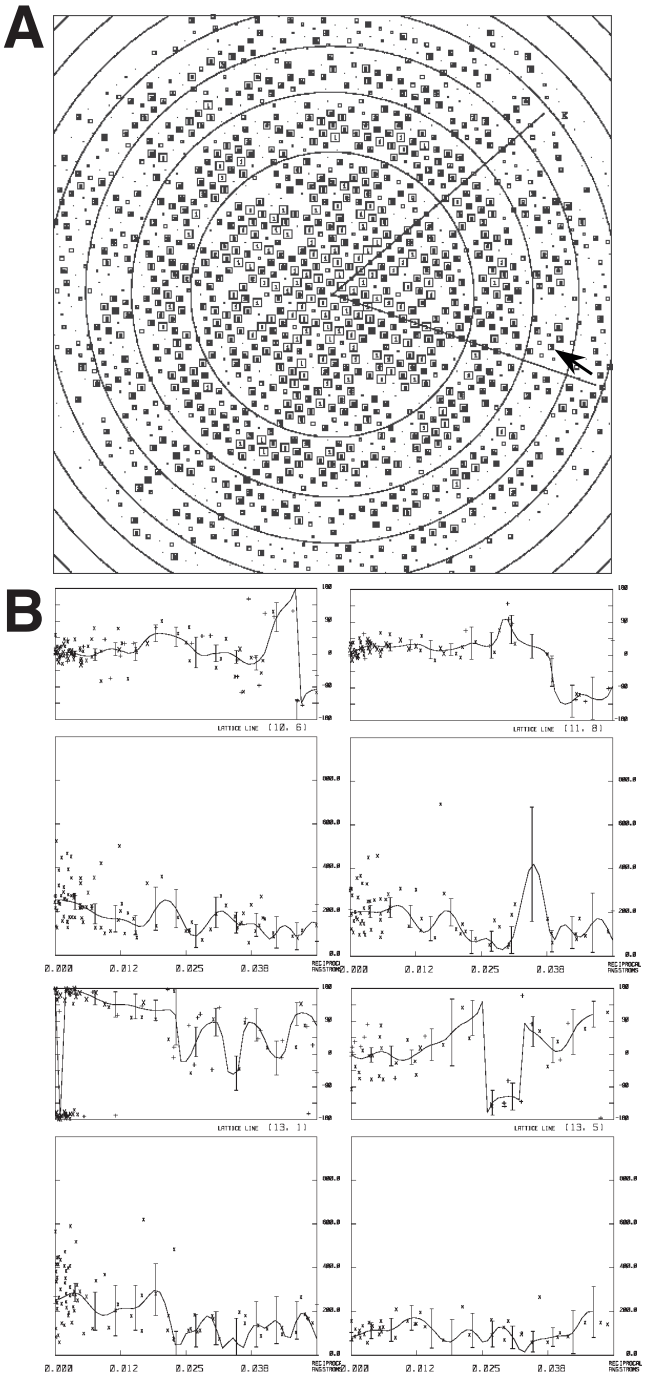

Figure S1. Calculated diffractions and lattice lines. (A) The calculated diffraction pattern of a frozen hydrated FimH-liganded mouse urothelial crystalline plaque. Each spot with a signal/noise ratio of greater than 1 is shown as a square; the size of the square is proportional to its signal/noise ratio. The number in each square is the 'IQ' number of the diffraction spot [IQ of 1 to 7 correspond to signal-to-noise ratio of 7 to 1, respectively [1]]. Circles are drawn at contrast transfer function (CTF) correction zeros; one spot at 7.9 Å (IQ=3) resolution is marked with an arrow. **(B)** The phase and amplitude variations along some of the high resolution lattice lines. The fitting curves were generated using the LATLINE program of the MRC software package.[2]

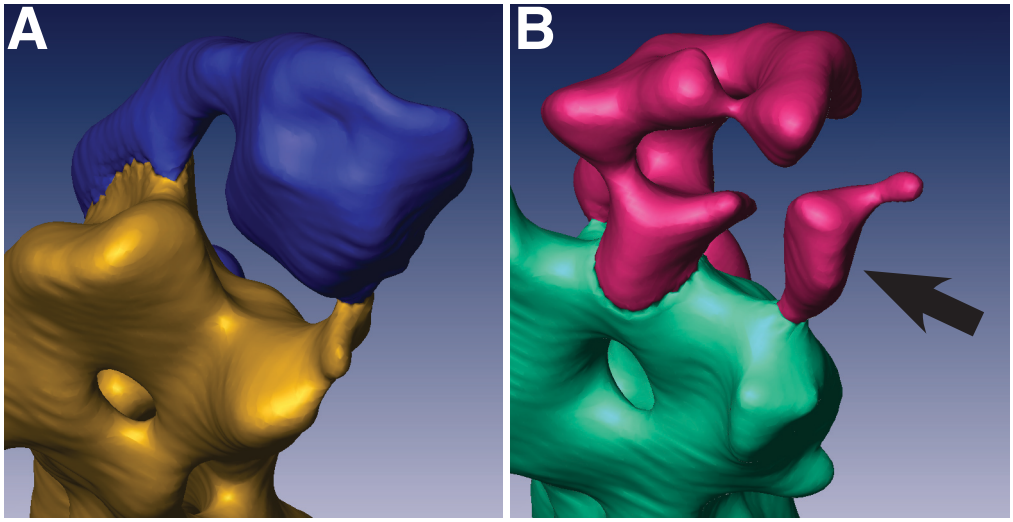

Figure S2. The putative FimH binding site on the 16 nm particle. Enlarged views (similar to that in Figs. 3E and 3F) of the FimH binding sites of the native (A) and FimH-bound (B) 16 nm particles. The density indicated by an arrow is potentially the residual density from FimH.

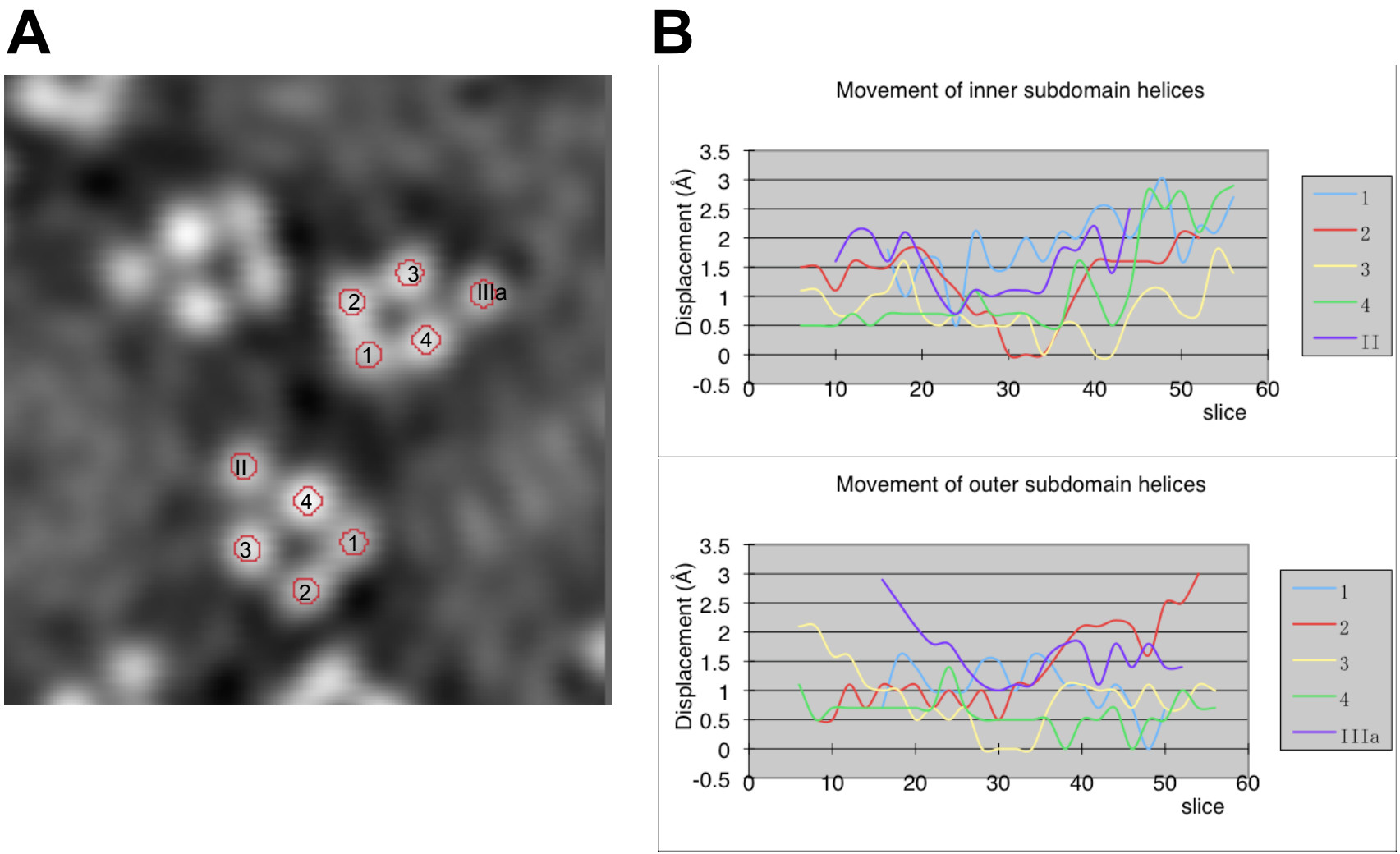

Figure S3. FimH-binding induced movement of the transmembrane helices of the uroplakins. To illustrate the movement of the transmembrane helices, we compared the electron density slices of the FimH-bound structure with that of the native structure, and measured the distances between the centers of the helices of the two structures. **(A)** A slice of the density map in the middle of the transmembrane domain of the FimH-bound 16-nm particle. Circles mark the center of the transmembrane helices in the segmentation process. **(B)** Displacement of the helices measured in the density slices of inner (upper) and outer (lower) subdomains. The x-axis represents the density map slices with larger numbers toward the cytoplasmic end. Note that the magnitudes of the displacement increase toward the both ends of the TM helices, suggesting the FimH-binding induced tilting (twisting) of the helices.

References for the Supplementary Data

1. Henderson, R., Baldwin, J. M., Ceska, T. A., Zemlin, F., Beckmann, E. & Downing, K. H. (1990). Model for the structure of bacteriorhodopsin based on high-resolution electron cryo-microscopy. J Mol Biol 213, 899-929.
2. Agard, D. A. (1983). A least-squares method for determining structure factors in three-dimensional tilted-view reconstructions. J Mol Biol 167, 849-52.